Active remote sensing observations for Cirrus Clouds profiling at subtropical and polar latitudes

Carmen Córdoba-Jabonero*[a], Eliane G. Larroza[b], Eduardo Landulfo[b], Walter M. Nakaema[b], Emilio Cuevas[c], Héctor Ochoa[d], Manuel Gil-Ojeda[a]

[a]Instituto Nacional de Técnica Aeroespacial (INTA), Atmospheric Research and Instrumentation Branch, Ctra. Ajalvir km.4, Torrejón de Ardoz-28850, Madrid, Spain; [b]Instituto de Pesquisas Energéticas e Nucleares (IPEN), Centro de Lasers e Aplicações, Sao Paulo, Brazil; [c]Agencia Estatal de Meteorología (AEMET), Atmospheric Research Centre of Izaña, Sta. Cruz de Tenerife, Spain; [d]Instituto Antártico Argentino/Dirección Nacional del Antártico (IAA/DNA), Buenos Aires, Argentina

ABSTRACT

Cirrus clouds with several important and climate-related applications are product of weather processes, and hence their occurrence and macrophysical/optical properties can vary significantly over different regions of the world. In this sense, a few case studies of cirrus clouds observed at both subtropical and polar latitudes are examined. Observations are carried out in three stations: Sao Paulo (Brazil, 23.6°S/46.8°W) and Sta. Cruz de Tenerife (Spain, 28.5°N/16.3°W), being both subtropical sites, and the Belgrano II base (Argentina, 78ºS/35ºW) in the Antarctic continent. Active remote sensing (LIDAR) is used for profiling measurements, and cirrus clouds features are retrieved by using a recently proposed methodology. Local radiosounding profiles are also used for cirrus-temperature correlation analysis. Optical and macrophysical properties (COD-cloud optical depth, top/base heights and Lidar Ratio, mainly) of both the subtropical and polar cirrus clouds are reported. This study is focused on the classification of the daily cloud features into three Cirrus COD-related categories: svCi-subvisual (COD < 0.06), stCi-semitransparent (0.06 < COD < 0.3), and opCi-opaque (COD > 0.3) clouds. In general, subtropical Cirrus clouds present lower LR values and are found at higher altitudes than those detected at polar latitudes. In addition, a higher svCi presence is observed over the polar station along the day, since svCi clouds are formed at lower temperatures.

Keywords: Cloud Optical Depth (COD), Cirrus clouds, LIDAR observations, Optical and Macrophysical properties, Polar Regions, Subtropical latitudes

*cordobajc@inta.es; phone +34 91 520 1294; fax +34 91 520 1317; www.inta.es/atmosfera

Remote Sensing of Clouds and the Atmosphere XIX; and Optics in Atmospheric Propagation and Adaptive Systems XVII, edited by Adolfo Comerón, Evgueni I. Kassianov, Klaus Schäfer, Richard H. Picard, Karin Stein, John D. Gonglewski, Proc. of SPIE Vol. 9242, 924203 · © 2014 SPIE · CCC code: 0277-786X/14/$18 · doi: 10.1117/12.2067306

1. INTRODUCTION

The influence of Cirrus clouds on weather and climate is actually an evident fact. Indeed, they can act as modulators in the radiation balance of the Earth-atmosphere system, and their heating or cooling effects can be observed at both regional and global scales[1]. However, the sensitivity of Cirrus clouds to factors associated with human-induced climate changes, i.e. greenhouse effect[2] and contamination of the upper troposphere from increasing aircraft traffic[3], is still poorly investigated. The climate-related changes in Cirrus cloud properties could alter (i.e., enhancing, opposing or even negating) the widely assumed global warming net effect related to the aerosols[4]. In particular, in a changing climate, cirrus induced by aircraft contrails would increase the upper tropospheric albedo and counteract the greenhouse gases warming effect[5]. The predominance of infrared greenhouse warming versus solar albedo cooling depends sensitively on both the altitudes and microphysical compositions of the Cirrus clouds[6]. Indeed, cloud height has an evident impact. Hence, high tropical Cirrus (i.e., formed from deep convection above warm moist layers) can be particularly effective greenhouse modulators. Conversely, lower Cirrus over Polar Regions could be more efficient for albedo effects. Thus, mid-latitude Cirrus clouds are assumed to reveal radiative implications varying with the season[7,8]. Moreover, Cirrus clouds are product of weather processes, and then their occurrence and macrophysical/optical properties can vary significantly over different regions of the world.

Since Cirrus clouds usually are located from 7 km height up to tropopause altitudes, active remote sensing techniques, mainly lidar systems, are usually used for detection of Cirrus clouds from ground-based[9,10] and space[11] observations. Lidars can provide height-resolved measurements with a relatively good both vertical and temporal resolutions, making them the most suitable instrumentation for high-cloud observations.

The aim of this work is to show the potential of lidar observations on Cirrus clouds detection in combination with a recently proposed methodology[12] to retrieve the Cirrus clouds macrophysical and optical features. In this sense, Cirrus clouds observations are performed in particularly located lidar stations at both subtropical and polar latitudes in order to establish a long-term Cirrus clouds monitoring over these stations in the future. In this preliminary step, a few case studies of Cirrus clouds observed over these subtropical and polar stations are presented. Their macrophysical, such as vertical extent, top/base heights and thickness, and optical, such as COD (Cloud Optical Depth) and Lidar Ratio (LR, extinction-to-backscatter ratio) properties are reported. Similarities/discrepancies found between them and climate implications are also discussed.

2. METHODOLOGY

2.1 Lidar observations of Cirrus clouds at subtropical and polar latitudes

Cirrus clouds observations used in this work are carried out in two subtropical sites and an Antarctic polar station. The Metropolitan city of Sao Paulo station (MSP, Brazil, 23.6°S 46.8°W) as managed by the Instituto de Pesquisas Energéticas e Nucleares (IPEN), and the Sta. Cruz de Tenerife observatory (SCO, Canary Islands-Spain, 28.5°N 16.3°W) by the Agencia Estatal de Meteorología (AEMET) are located at subtropical latitudes. The Antarctic Belgrano II base (BEL, Argentina, 78ºS 35ºW) is managed by the Dirección Nacional del Antártico (DNA).

In SCO and BEL sites are running in routine operation two Micropulse Lidars, v.3 (MPL-3) and v.4 (MPL-4, including depolarization capability), respectively. They are standards of those are within the NASA/MPLNET (MicroPulse Lidar NETwork, mplnet.gsfc.nasa.gov), managed by the Spanish Institute for Aerospace Technology (INTA, Instituto Nacional de Técnica Aeroespacial, www.inta.es/atmosfera) in collaboration with the AEMET (Spain) and DNA (Argentina), respectively. The lidar system operating in the MSP station (SPL) is managed by the IPEN/Centro de Lasers e Aplicaçoes (IPEN/CLA, www.ipen.br), and belongs to LALINET a.k.a. ALINE (Latin America LIdar NETwork, lalinet.org). Main lidar characteristics are shown in Table 1. Specific instrumental features related to the applied retrieval algorithm (see next Section), as range-corrected signal, backscattering ratio, optimal threshold function, among others, for each lidar system used in this work are examined.

Lidar profiles are selected in the basis of cirrus signal detected at above 7 km height. In the case of polar Cirrus, the detection range is limited up to 15 km height in order to avoid PSC (Polar Stratospheric Clouds) contamination. Radiosounding profiles are also used in this analysis for Cirrus temperature estimation. In this preliminary study, one Cirrus case is presented for each station. An on-going work is being performed devoted to a more extended dataset with Cirrus detection retrieval in all these stations.

Table 1. Main characteristic of the three lidar systems used in this work, together the acquisition information.

Lidar system	SPL	MPL-3	MPL-4
Station	MSP (23.6°S 46.8°W, 660 m a.s.l.)	SCO (28.5ºN 16.2ºW, 52 m a.s.l.)	BEL (77.9ºS 35.0ºW, 256 m a.s.l.)
Routine operation	Yes	Yes	Yes
Networks	LALINET/ALINE	MPLNET SPALINET	---
Wavelength (nm)	532	523	527
Energy/pulse (mJ)	150 - 330	0.007 (max.)	0.010 (max.)
Pulse repetition frequency (Hz)	10 – 20	2500	2500
Eye-safe	No	Yes	Yes
Depolarization	No	No	Yes
Raman capability	Yes	No	No
Vertical resolution	3.75 m	75 m	75 m
Integrating time	1 - 2 min	1 min	1 min

2.2 Retrieval algorithm for macrophysical and optical properties of Cirrus clouds

Both macrophysical and optical properties of the Cirrus clouds are retrieved from lidar measurements by using the methodology reported in Larroza et al. (2013)[12]. However, the determination of both the base and the top height-levels, z^{base} and z^{top}, respectively, of the Cirrus cloud layer is differently performed from that shown in that work[12]. In our study, the expression used for the threshold function $thR(z)$, which clearly can differentiate the lower and higher limits of the "attenuated" backscattering ratio $R^{att}(z)$ profile within the Cirrus cloud layer due to the sharpness of the $R^{att}(z)$ profile respect to Rayleigh backgrounds in both the cloud limits, is

$$thR(z) = 1 + a \cdot R^{att}(z), \tag{1}$$

where a is a parameter ranging between 0 and 1, which provides the percentage degree of $R^{att}(z)$ regarding $thR(z)$ is higher than Rayleigh background ($R^{att}(z < z_1)$ =1), and $R^{att}(z)$ is defined as

$$R^{att}(z) = R(z) \cdot T^2(z) = \frac{\beta(z)}{\beta_m(z)} \cdot T^2(z) = \frac{\beta^{att}(z)}{\beta_m(z)}, \tag{2}$$

being $R(z)$ the backscattering ratio, $T(z)$ the transmittance due to molecules (Rayleigh) and aerosols, $\beta(z)$ and $\beta_m(z)$ the backscatter and molecular coefficients, respectively, and $\beta^{att}(z)$ $(= \beta(z)T^2(z))$ the "attenuated" backscatter coefficient. Then, z^{base} and z^{top} are found under the condition that the difference between $R^{att}(z)$ and $thR(z)$ is higher than a given value b at both base and top cloud height-levels, respectively. The definition of this threshold function $thR(z)$ and, in particular, the designation of a given value to the parameter a and the difference factor b, depend on lidar systems and their measurements. In particular, optimal a and b values of 0.1 (10%) and 0.5, respectively, were applied for each lidar system.

Among the macrophysical features, the vertical extent, the top and base heights and the thickness are obtained. The optical properties retrieved, considering also multiple scattering effects introduced in the retrieval algorithm[12], are the

Cloud Optical Depth (COD) and Lidar Ratio (LR, extinction-to-backscatter ratio). These all parameters are examined for the selected case studies of both the subtropical and polar Cirrus clouds.

3. RESULTS

3.1 Subtropical Cirrus clouds features

3.1.1 Cirrus case over SCO station

A Cirrus cloud was observed over SCO site during late autumn on 26 November 2009. Hourly-averaged profiles are analyzed along the day. Macrophysical and optical features are retrieved from these hourly-averaged lidar profiles by using the proposed methodology (see Sect. 2.2) for this case study. The backscattering ratio $R(z)$ with the corresponding values of LR and COD are obtained. In dependence on the COD (τ), Cirrus profiles are classified into three categories: sub-visual (svCi, $\tau < 0.06$), semi-transparent (stCi, $0.06 < \tau < 0.3$), and opaque (opCi, $\tau > 0.3$). Figure 1 shows the temporal evolution of the backscattering ratio $R(z)$ for Cirrus clouds observed at SCO site along the day on 26 November 2009, highlighting the Cirrus classification found. Results indicate a progressive drift into larger COD values together to a lowering of the base and top heights of the Cirrus clouds is observed.

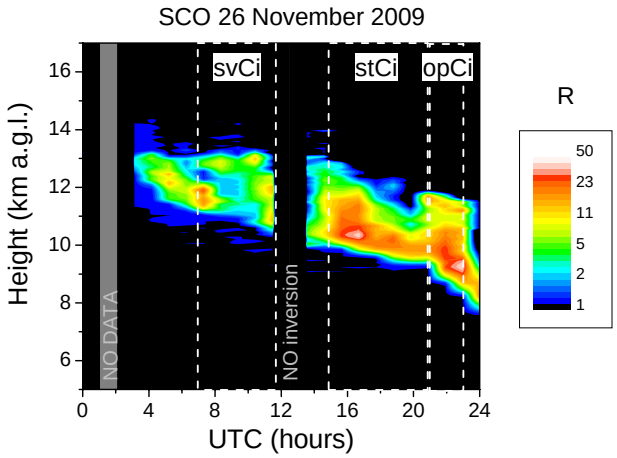

Figure 1. Temporal evolution of Cirrus clouds observed over SCO site on 26 November 2009 in terms of the backscattering ratio (R). The three Cirrus categories (svCi-subvisual, stCi-semitransparent and opCi-opaque) found for this day are also shown.

The correlation of the LR and both the top and base heights of the Cirrus clouds respect to the COD is also examined. Figure 2 shows the retrieved LR values together the z^{base} and z^{top} heights as a function of COD. LR values lower than 10 sr are found for svCi, being higher LR for the other stCi and opCi but no larger than around 15 sr. z^{base} are higher than 10 km heights for the svCi, and ranging from 8 to 10 km height for stCi and opCi. In addition,svCi reach higher z^{top} altitudes, being between 12.5 and 14 km, while stCi and opCi z^{top} are found between 11 and 12.5 km height. In general, as results show, LR values are lower for svCi and they are found at higher altitudes than for the other stCi and opCi clouds.

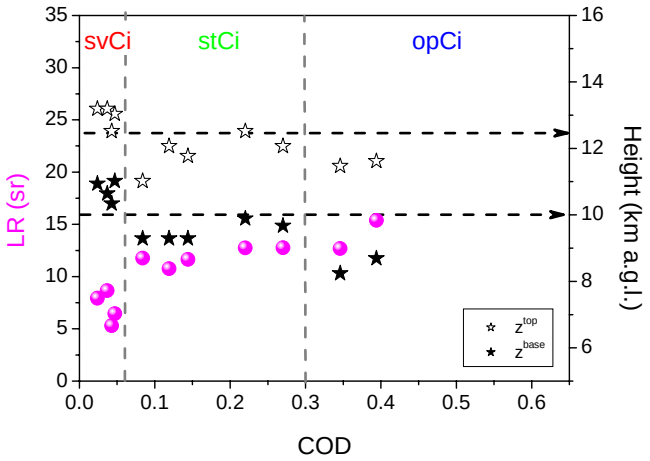

Figure 2. Lidar Ratio (LR) values (solid circles) and both top and base heights (open and full stars, respectively) obtained for the Cirrus clouds observed over SCO site on 26 November 2009. The three Cirrus categories: svCi-subvisual (red), stCi-semitransparent (green) and opCi-opaque (blue) are also marked.

In addition, the correspondence between the backscattering ratio $R(z)$ for these three Cirrus categories and the temperature profile obtained from local radiosoundings is also analyzed. Figure 3 shows both the $R(z)$ and temperature profilings, indicating several temperature thresholds for water/ice phase dominance levels inside the clouds. Shaded bands show that svCi are formed at lower temperatures (mostly < -50ºC) than the other stCi and opCi categories, being the tropopause located at around 13.5 km height.

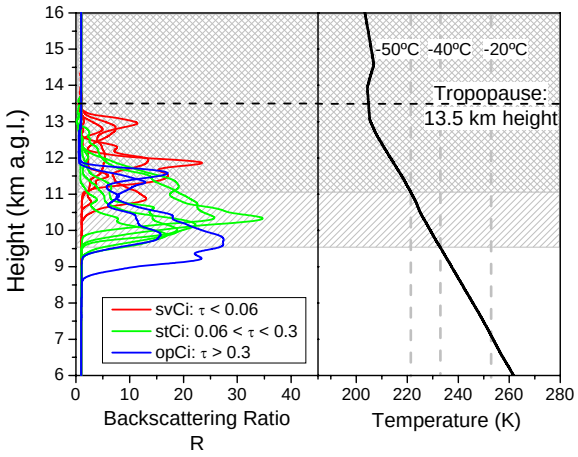

Figure 3. Cirrus clouds observed over SCO site on 26 November 2009: (Left) The backscattering Ratio (R) in dependence on the COD (τ) retrieved, and (right) the temperature profile obtained from local radiosoundings (right). Cirrus clouds are divided into sub-visual (svCi, red lines), semitransparent (stCi, green lines) and opaque (opCi, blue lines) categories.

3.1.2 Cirrus case over MSP station

In the case of the Cirrus clouds observed over MSP site during early austral winter on 11 June 2007 (case also examined in Larroza et al. (2013)[12]), SPL profiles registered for a few hours are analyzed. As in the previous case, macrophysical and optical features are derived by using the same methodology (see Sect. 2.2). Both LR and COD values are retrieved,

and the $R(z)$ profiles for Cirrus clouds are shown in Figure 4. Results indicate a layered structure composed of one or two layers with alternating COD values between stCi and opCi clouds, but no svCi are observed for this case.

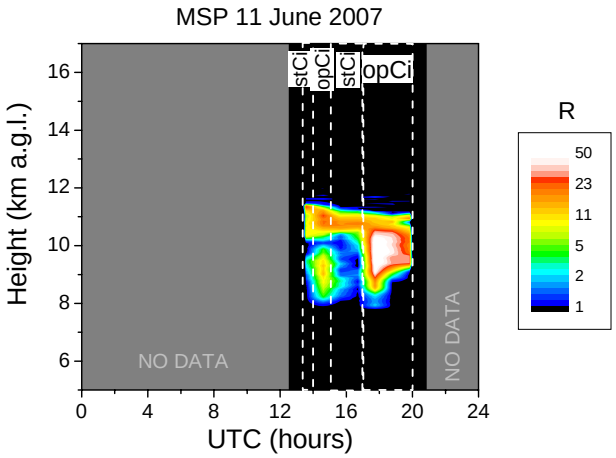

Figure 4. The same as for Fig.1, but over MSP station on 11 June 2007 in terms of the backscattering ratio (R). The two Cirrus categories (stCi-semitransparent and opCi-opaque) found for this day are also shown.

As previously, a correlation study of LR and both z^{base} and z^{top} versus COD values is also examined and shown in Figure 5. First, it can be observed that as LR decrease as COD increase: LR values of 25-30 sr and 10-20 sr are found for stCi and opCi, respectively. z^{base} is between 8 and 9 km and z^{top} around 11 km height for all the Cirrus cases observed. In general, LR values are higher for stCi than for opCi clouds, but their occurrence is found at similar altitudes between 8 and 11 km height.

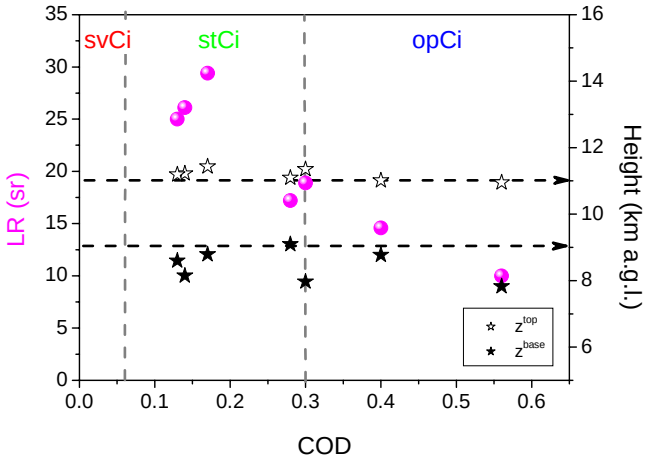

Figure 5. The same as for Fig.2, but over MSP station on 11 June 2007. Cirrus categories: svCi (red), stCi (green) and opCi (blue) are also marked.

In addition, Figure 6 shows the vertical structure of the $R(z)$ together the temperature profile registered for this case. As previously, shaded bands show that stCi and opCi clouds are mostly formed at temperatures ranging from -50ºC to -30ºC, with a lower tropopause height (around 12.5 km) than that observed in the SCO case.

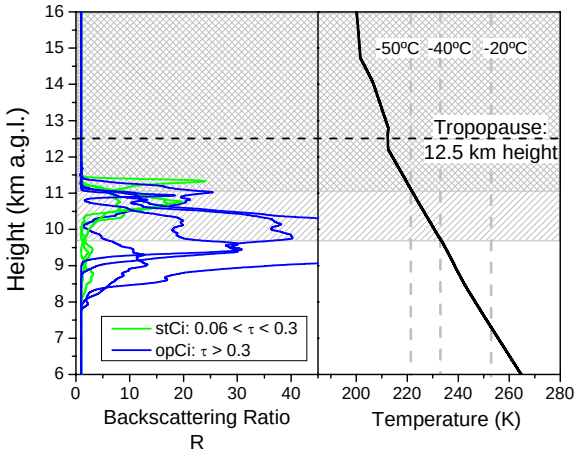

Figure 6. The same as for Fig. 3, but over MSP station on 11 June 2007. Cirrus clouds are divided into stCi (green lines) and opCi (blue lines) categories.

3.2 Polar Cirrus clouds features

A Cirrus cloud was observed over BEL base during late austral autumn on 22 May 2010, and hourly-averaged profiles are analyzed along the day. As in the previous cases, macrophysical and optical features are also retrieved, and the same Cirrus categories (svCi, stCi and opCi) are examined. Figure 7, as for Figs. 1 and 4, shows the temporal evolution of the backscattering ratio $R(z)$ for Cirrus clouds observed at BEL site along the day on 22 May 2010 (Cirrus classification is also included). Results indicate that opCi are observed for the first two hours, followed by svCi and stCi occurrence, but with COD values for stCi clouds close to 0.08 (almost within the COD range designated to svCi). In overall, Cirrus persist at similar height levels along the day, and no lowering of Cirrus is observed (unfortunately, no data were available from 16:00 UTC on).

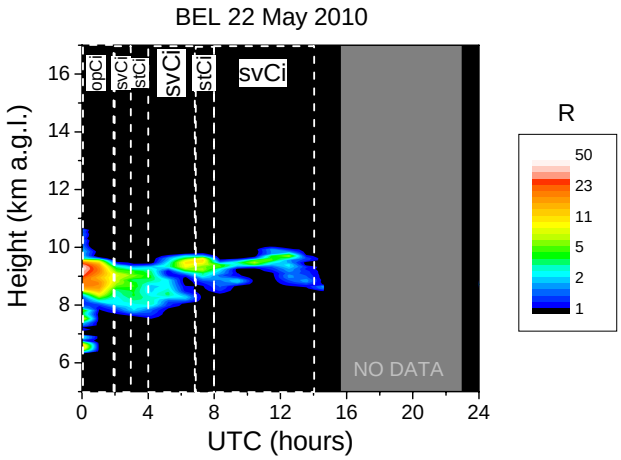

Figure 7. The same as for Fig.1, but over BEL station on 22 May 2010 in terms of the backscattering ratio R. The two Cirrus categories (svCi-subvisual and opCi-opaque) found are also shown for this day.

The LR correlation with the COD is also examined, as previously. Figure 8 shows the retrieved LR values together the z^{base} and z^{top} heights as a function of COD for this case. It must be noted that LR values for svCi (including the low COD-stCi) are definitely increasing from 15 up to a maximum value of 32 sr, while opCi clouds present LR values around 30 sr. z^{base} and z^{top} altitudes, respectively, are higher than 7 km and 9 km height up to the tropopause level, for

all svCi, stCi and opCi clouds. In general, these results show LR values for polar Cirrus clouds higher than those obtained in the subtropical SCO case, independently on the COD, and similar to those derived for the MSP case but with a contrary behavior respect to the COD. In addition, they are also found at lower altitudes, as expected for polar latitudes.

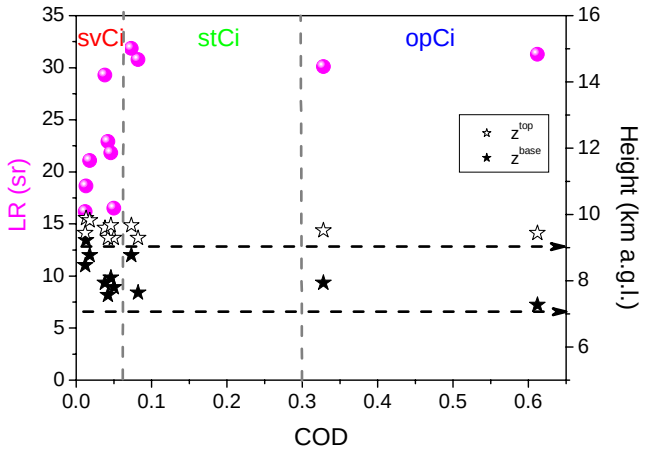

Figure 8. The same as for Fig.2, but over BEL station on 22 May 2010. The Cirrus categories: svCi (red), stCi (green) and opCi (blue) are also marked.

As previously in the two subtropical cases, the correspondence between the backscattering ratio $R(z)$ for these three Cirrus categories and the temperature profile obtained from local radiosoundings is also analyzed. Figure 9 shows both the $R(z)$ and temperature profilings, indicating several temperature thresholds for water/ice phase dominance levels inside the clouds. Shaded bands show that all the Cirrus clouds present for this day, svCi (also stCi) and opCi, are formed at lower temperatures than for both the subtropical cases (see Sect. 3.1).

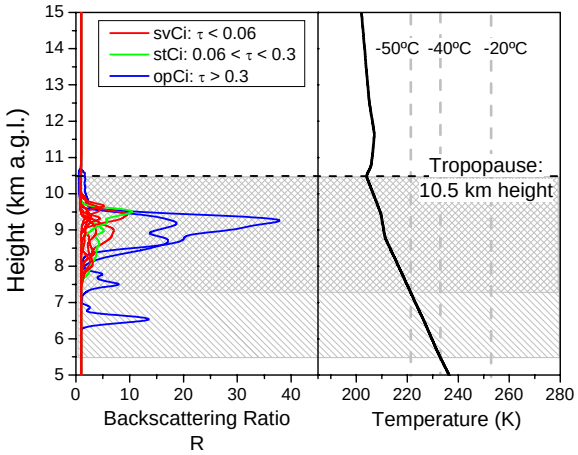

Figure 9. The same as for Fig.3, but over BEL station on 22 May 2010. Cirrus clouds are divided into svCi (red lines), stCi (green lines) and opCi (blue lines) categories.

4. CONCLUSIONS

Cirrus clouds have been analyzed in terms of their macrophysical and optical properties as retrieved by a recently developed methodology applied to lidar measurements. As a preliminary step, a few case studies of Cirrus clouds

observed at subtropical and polar latitudes are presented in this work. These cases correspond to two subtropical Cirrus clouds detected over both SCO and MSP stations on 26 November 2009 (late autumn) and 11 June 2007 (early austral winter), respectively, and one polar Cirrus cloud over the Antarctic BEL base on 22 May 2010 (late austral autumn). Their backscattering ratio (R) profiles together with their top and base height levels, Cloud Optical Depth (COD) and Lidar Ratio (LR) have been reported.

This study has been focused on the classification of the daily cloud features into three Cirrus categories in relation with the COD: svCi-subvisual (COD < 0.06), stCi-semitransparent (0.06 < COD < 0.3), and opCi-opaque (COD > 0.3). They have been compared regarding the values found of their LR and both the top and base heights with respect to the COD for each Cirrus category. In addition, an analysis of their correlation with the temperature of the atmosphere has been also performed.

Subtropical svCi and opCi clouds present LR values lower than 10 sr and between 10-20 sr, respectively, while they are higher for polar Cirrus clouds, indeed, LR for svCi and opCi are ranging from 15 to 30 sr and around 30 sr, respectively; stCi are a mixed case between them. Regarding their altitudes, suptropical svCi are located higher than opCi clouds, ranging, respectively, from 10 and 8 km height up to tropopause height-levels. However, the presence of Polar Cirrus is observed, in general, at lower altitudes than those for the subtropical cases up to the tropopause, situated at lower heights, as expected in Polar Regions. This is also related to the thermodynamic structure of the atmosphere, since svCi clouds are formed at lower temperatures (< -50ºC) at both latitudes, and they are reached at higher altitudes. In addition, subtropical opCi, however, are formed between -50ºC and -30ºC, while polar ones at < -50ºC as for svCi. Indeed, as expected, a higher svCi presence is observed over the polar station during the day, since svCi clouds are formed at lower temperatures, as those observed at polar latitudes.

It should be noted that results obtained are specific for those particular cases analyzed in this preliminary work. However, in general, subtropical Cirrus clouds present lower LR values and are found at higher altitudes than those detected at polar latitudes. Similarities and differences can be plausibly provided, as long as a larger dataset can be available to be analyzed in each station.

In addition, such considerations can improve the treatment of the different latitude-types of Cirrus clouds to be introduced in large-scale models for climate-related issues, as well as be useful in validation assessments of the retrieval of their properties from satellites (i.e., next future ESA/EarthCARE and Sentinels missions).

ACKNOWLEDGEMENTS

This work is supported by the Spanish Ministerio de Economía y Competitividad (MINECO) under grant CGL2011-24891 (AMISOC project). Authors thank the staff of all the stations responsible for instrumentation maintenance and support. C. C.-J. thanks the Fundação de Amparo à Pesquisa do Estado de São Paulo (FAPESP) for their support under grant 2013/11836-2 during her research stay in the Instituto de Pesquisas Energéticas e Nucleares (IPEN).

REFERENCES

[1] Liou, K.-N., “Influence of cirrus clouds on weather and climate processes: A global perspective,” Mon. Weather Rev. 114, 1167-1200 (1986).
[2] Iacono, M. J., J. S. Delamere, E. J. Mlawer, M. W. Shephard, S. A. Clough, and W. D. Collins, “Radiative forcing by long-lived greenhouse gases: Calculations with the AER radiative transfer models,” J. Geophys. Res. Atmos. 113, D13103 (2008).
[3] Boucher, O., “Air traffic may increase cirrus cloudiness,” Nature 397, 30-31 (1999).
[4] Boucher, O., D. Randall, P. Artaxo, C. Bretherton, G. Feingold, P. Forster, V.-M. Kerminen, Y. Kondo, H. Liao, U. Lohmann, P. Rasch, S.K. Satheesh, S. Sherwood, B. Stevens and X.Y. Zhang, “Clouds and Aerosols”. In: Climate Change 2013: The Physical Science Basis. Contribution of Working Group I to the Fifth Assessment Report of the Intergovernmental Panel on Climate Change [Stocker, T.F., D. Qin, G.-K. Plattner, M. Tignor, S.K. Allen, J. Boschung, A. Nauels, Y. Xia, V. Bex and P.M. Midgley (eds.)]. Cambridge University Press, Cambridge, United Kingdom and New York, NY, USA (2013).

[5] Burkhardt, U. and Kärcher, B., "Global radiative forcing from contrail cirrus," Nature Climate Change 1, 54-58 (2011).
[6] Myhre, G., D. Shindell, F.-M. Bréon, W. Collins, J. Fuglestvedt, J. Huang, D. Koch, J.-F. Lamarque, D. Lee, B. Mendoza, T. Nakajima, A. Robock, G. Stephens, T. Takemura and H. Zhang, "Anthropogenic and Natural Radiative Forcing". In: Climate Change 2013: The Physical Science Basis. Contribution of Working Group I to the Fifth Assessment Report of the Intergovernmental Panel on Climate Change [Stocker, T.F., D. Qin, G.-K. Plattner, M. Tignor, S.K. Allen, J. Boschung, A. Nauels, Y. Xia, V. Bex and P.M. Midgley (eds.)]. Cambridge University Press, Cambridge, United Kingdom and New York, NY, USA (2013).
[7] Sassen, K., and J. Comstock, "A Midlatitude Cirrus Cloud Climatology from the Facility for Atmospheric Remote Sensing. Part III: Radiative Properties," J. Atmos. Sci. 58(5), 2113–2127 (2001).
[8] Dupont, J.-C., and M. Haeffelin, "Observed instantaneous cirrus radiative effect on surface-level shortwave and longwave irradiances," J. Geophys. Res. 113, D21202, doi:10.1029/2008JD009838 (2008).
[9] Sassen, K., and J. R. Campbell, "A midlatitude cirrus cloud climatology from the Facility for Atmospheric Remote Sensing. Part I: Macrophysical and synoptic properties," J. Atmos. Sci. 58, 481-496 (2001).
[10] Dupont, J.-C., M. Haeffelin, Y. Morille, V. Noël, P. Keckhut, D. Winker, J. Comstock, P. Chervet, and A. Roblin, "Macrophysical and optical properties of midlatitude cirrus clouds from four ground-based lidars and collocated CALIOP observations," J. Geophys. Res. 115, D00H24, doi:10.1029/2009JD011943 (2010).
[11] Sassen, K., Z. Wang, and D. Liu, "Global distribution of cirrus clouds from CloudSat/Cloud-Aerosol Lidar and Infrared Pathfinder Satellite Observations (CALIPSO) measurements," J. Geophys. Res. 113, D00A12, doi:10.1029/2008JD009972 (2008).
[12] Larroza, E.G., Nakaema, W. M., Bourayou, R., Hoareau, C., Landulfo, E. and Keckhut, P., "Towards an automatic lidar cirrus cloud retrieval for climate studies," Atmos. Meas. Tech. 6, 3197-3210 (2013).